

Simulation of Particle Release for Diffusing Alpha-Emitters Radiation Therapy

Dmytro Fedorchenko^{a,*}, Shlomi Alani^a

^a*Ziv Medical Center, Derech HaRambam, Zefat, 13100, Israel*

Abstract

We used Monte Carlo simulations to study release of radium-224 daughter nuclei from the seed used for Diffusing Alpha-Emitters Radiation Therapy (DART). Calculated desorption probabilities for polonium-216 (15%) and lead-212 (12%) showed that they make a significant contribution to total release from the seed. We also showed that the dose to tissue from decays inside the 10mm long seed exceeds 2.9 Gy for initial radium-224 activity of 111 kBq.

Keywords:

Monte Carlo simulation, Radium-224, Alpha-particle therapy

1. Introduction

Radiation therapy using alpha particles is considered a very promising approach in treatment of malignant tumors. Alpha particles, having high linear energy transfer (LET) and a range of 50-100 μm in human tissue, provide excellent possibilities for highly localized tumor treatment. The traditional approach to alpha therapy implies usage of radionuclides emitting single alpha particle, such as, for example, ^{213}Bi , ^{221}At and ^{212}Pb . More advanced techniques called in vivo generators [1] use decay chains where several alpha particles are emitted. Radionuclides ^{225}Ac , ^{224}Ra and ^{223}Ra with four alpha particles in the decay chain are considered as prospective candidates for such an approach.

*Corresponding author

Email addresses: d.fedoechenko@gmail.com (Dmytro Fedorchenko),
shlomialani@me.com (Shlomi Alani)

Short alpha particle range requires targeted delivery of the mother radionuclide to the tumor tissue for the efficient treatment. This could be achieved by using specific radiolabeled compounds acting as targeting agents. However, in the case of in vivo generators tumor targeting using labeled agents is complicated because of nuclear recoil effect [2]. Alpha-decay of the mother nucleus produces a daughter nucleus with kinetic energy of 100-200 keV which is enough to break chemical bonds and to leave the targeting agent molecule.

The possible solution to the problem is local administration of alpha-emitting radionuclide directly into the tumor volume. The example of such an approach is diffusing alpha-emitters radiation therapy (DART) [3, 4, 5, 6, 7]. According to this method thin seeds impregnated by ^{224}Ra are placed inside the tumor. Decay of ^{224}Ra nucleus produces alpha particle and ^{220}Rn recoil nucleus (Figure 1). The recoil nucleus gains enough energy to leave the thin radium-impregnated surface layer of the DART seed. Diffusion of the released daughter nuclei forms the treatment volume of several millimeters with high alpha particles dose. At the same time radiotoxic radium nuclei remain within the seed. Clinical trials of DART showed promising results for treatment of several types of tumors [7].

The comprehensive theoretical model describing the long-range dynamics of recoil nuclei escaping the DART seed was developed by Arazi [5]. The model is based on the system of diffusion equations with terms describing nuclei sources and decay. Solution of this system gives concentrations of the nuclei released from the needle on the distances of several millimeters.

However, within the macroscopic approach it is impossible to describe release of the recoil nuclei from the DART seed. This process requires detailed microscopic description because recoil nuclei emerging in a thin surface layer undergo only a small number of interatomic interactions before escaping the seed.

The aim of this work was to study transport of recoil nuclei emerging from radionuclide decay of ^{224}Ra and its daughter nuclei using Monte Carlo simulation. Our model included simulation of radioactive decay processes with subsequent detailed simulation of daughter nuclei and decay products transport.

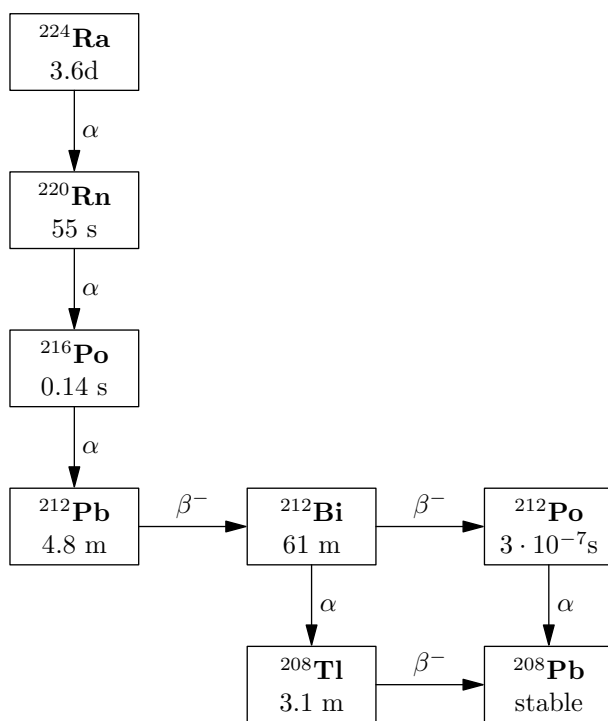


Figure 1: ^{224}Ra decay chain

2. Monte Carlo simulation setup

For the simulations of radioactive decay and transport processes we used GEANT4 simulation toolkit version 11.02 [8, 9, 10]. The toolkit has a very flexible architecture based on a collection of C++ classes covering various aspects of particle transport simulation. This allows selection and customisation of physical models to satisfy requirements of the particular problem.

Simulation of the recoil nuclei transport in the thin surface layer of DART seed requires usage of appropriate physical models. The main physical process responsible for the transport is ion elastic scattering and only a small number of collisions occur in a thin layer. In this case one needs an accurate simulation of individual collisions with realistic interatomic potential. The standard models of ion elastic scattering used by GEANT4 are based on multiple scattering (MSC) approximation [11]. This approximation uses the statistical approach valid only when the moving particle undergoes a significant number of collisions and in the case of a nanometer-thick layer this condition is not satisfied.

Instead of MSC model we used an accurate single scattering model developed by Mendenhall and Weller [12], and later implemented for GEANT4 toolkit as a G4ScreenedNuclearRecoil class [13]. This model considers classical pair interactions of the moving ions with screened Coulomb potential. Simulations of ion scattering in thin foils and ion implantation showed perfect agreement of the model with the experimental data [13].

The DART seed was simulated as a solid cylinder with diameter of 0.3 mm and length of 10 mm. The seed dimensions correspond to those used for theoretical and experimental research [3]. Seed material was stainless steel with element composition taken from the GEANT4 material database: Fe - 74%, Cr - 18%, Ni - 8% .

3. Results and discussions

3.1. Simulation of ^{220}Rn release from impregnated layer

The key parameter of the DART seed model is thickness of the radium-impregnated layer. This parameter determines the decay products release from the DART seed. To determine the realistic thickness value we used the available data on ^{220}Rn release [5]. According to these experimental studies ^{220}Rn desorption probability is $40\pm 4\%$. This value could be used to estimate

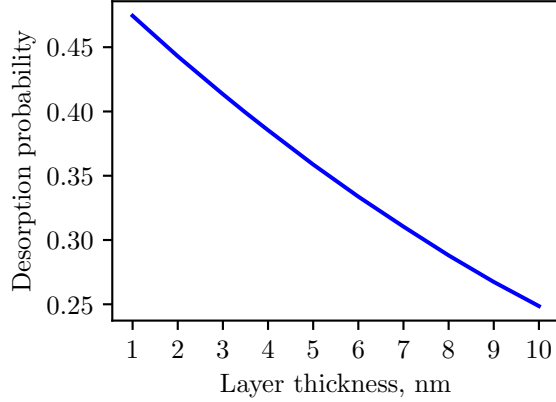


Figure 2: Calculated ^{220}Rn desorption probability for different thickness of radium-impregnated surface layer of the DART seed

thickness of the impregnated layer by evaluating ^{220}Rn release for different layer thicknesses.

Simulation of the impregnated layer was performed by placing ^{224}Ra ions in random positions within the surface layer of the DART seed of the given thickness. After that decay of these was simulated and ^{220}Rn were transported in the seed volume. The desorption probability was calculated as a ratio of ^{220}Rn nuclei crossing the seed surface to the number of decayed ^{224}Ra nuclei.

The calculated values of ^{220}Rn desorption probability for different thicknesses of the impregnated layer are presented in Figure 2. According to the obtained dependency ^{220}Rn desorption probability of 40% corresponds to 3.5 nm thick impregnated layer. This layer thickness was used for subsequent simulations of the radioactive decay products transport.

3.2. Simulation ^{224}Ra decay products transport inside the seed

Simulation ^{224}Ra decay products transport inside the seed Radon is not the only member of the radium decay chain that is released from the DART seed. Other nuclei from ^{224}Ra decay chain also gain enough recoil energy to escape the seed body. These escaped nuclei affect the dose distribution around the seed.

The important factor that determines release of ^{224}Ra decay products from the DART seed is their distribution inside the seed. This distribution

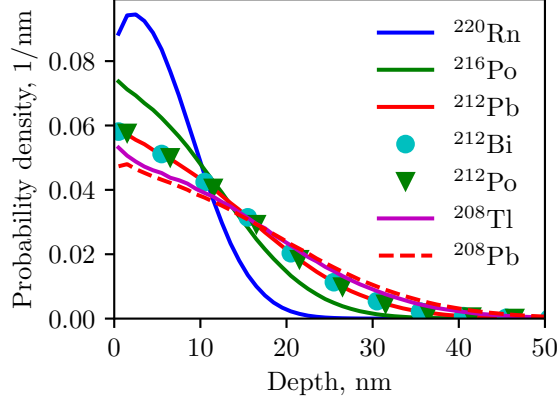


Figure 3: Spatial distribution of radionuclides belonging to ^{224}Ra decay chain inside the seed.

is formed by recoil nuclei traveling from the surface layer impregnated by ^{224}Ra . Part of these nuclei escapes from the seed, but the remaining part travels away from the surface. Recoil energy of about 100 keV gained from alpha decays in the decay chain allows the emerging daughter nuclei to penetrate deeper into the seed. For beta decay the recoil energy is small and displacements of the emerging nuclei from the point of decay are small.

For the simulation we randomly placed ^{224}Ra nuclei in the 3.5 nm thick surface layer, and simulated decays and subsequent transport of all of its daughter nuclei. Figure 3 shows the spatial distribution of recoil nuclei inside the seed obtained from the Monte Carlo simulation. These distributions could be characterized by an average depth at which the recoil nuclei are located in the seed body. Table 1 contains the average depths calculated using the spatial distributions.

The calculated distributions show that every next nuclei in ^{224}Ra decay chain penetrate deeper into the seed forming the elongated distribution tail. While for ^{220}Rn nuclei the distribution spreads up to 25 nm depth with average depth of 6.3 nm, ^{208}Pb nuclei could travel up to 50 nm from the surface with average depth of 13.8 nm. For beta decay products ^{212}Bi and ^{212}Po displacement from the point of decay is small and their spatial distributions almost coincide with the distributions of the corresponding parent nuclei, and have almost equal average depths.

Table 2 contains desorption probabilities for the ^{224}Ra daughter nuclei

Nucleus	Depth, nm
^{220}Rn	6.278
^{216}Po	8.843
^{212}Pb	11.232
^{212}Bi	11.252
^{212}Po	11.306
^{208}Tl	12.926
^{208}Pb	13.778

Table 1: Average depths of ^{224}Ra daughter nuclei in the DART seed

Nucleus	Release fraction
^{220}Rn	0.398710
^{216}Po	0.149228
^{212}Pb	0.120938
^{212}Bi	0.001048
^{212}Po	0.0022797
^{208}Tl	0.032602
^{208}Pb	0.0765695

Table 2: Desorption probabilities of ^{224}Ra daughter nuclei

obtained from the Monte Carlo simulation. The desorption probabilities are calculated as ratios of the number of nuclei of particular sort leaving the seed to the number of decayed ^{224}Ra nuclei. One can see ^{220}Rn has the highest desorption probability of 40%, however, desorption probabilities for ^{216}Po (15%) and ^{212}Pb (12%) are also significant for formation of dose distribution around the seed.

The high desorption probability of ^{220}Ra nuclei is determined by the distribution of the parent ^{224}Ra nuclei, which is assumed to be uniform and confined to a 3.5 nm thick surface layer. For such distribution the average depth is 1.75 nm and escape probability of emerging ^{220}Rn nuclei is rather high. Distribution of its immediate daughter ^{220}Rn has a much larger depth of 6.3 nm (see Table 1) that results in a substantially lower desorption probability for ^{216}Po . The average depth of ^{216}Po nuclei distribution inside the seed does not differ considerably from that of ^{220}Rn and both radionuclides have similar desorption probabilities.

The low recoil energy of beta-decay products ^{212}Bi and ^{212}Po results in

their short ranges in seed material. In this case the range defines the thin surface layer from which escape of the recoil nuclei is possible. From Figure 3 one could see that only a small part of ^{212}Bi and ^{212}Po are located in such a surface layer and could actually leave the seed volume. The corresponding desorption probabilities are very low compared to those of the alpha decay products. The difference in desorption probabilities between ^{212}Bi and ^{212}Po could be understood from the Q-values of the corresponding beta decays: 569.9 keV for ^{212}Pb decay and 2252.1 keV for ^{212}Bi decay [14]. The higher Q-value and higher recoil energy of ^{212}Po nuclei results in higher desorption probability.

Desorption probability for ^{208}Tl is low in comparison to other alpha decay products belonging to the ^{224}Ra decay chain. The reason for this is that the probability of alpha decay of its parent nucleus is only 35.9% (Figure 1) and a smaller number of ^{208}Tl nuclei is produced.

Stable radionuclide ^{208}Pb is produced by beta decay of ^{208}Tl and alpha decay of ^{212}Po . The recoil energy gained from the latter process determines the desorption probability for ^{208}Pb , because the probability of ^{208}Pb nuclei escaping after beta decay is very small. The parent radionuclide ^{212}Po is produced with the probability of 64.1%, and this is also the fraction of ^{208}Pb nuclei produced from alpha decay and having a reasonable escape probability. This results in the relatively low ^{208}Pb desorption probability compared to desorption probabilities of other decay chain members produced from alpha decay.

3.3. Simulation of recoil nuclei transport in tissue

The range of recoil nuclei in tissue is determined by their spectra on the seed-tissue border. Figure 4 shows calculated spectra of the recoil nuclei that escape the seed and enter the surrounding tissue. The figure does not include beta decay products ^{212}Bi and ^{212}Po because due to low recoil energy they have a very short range in tissue.

The calculated spectrum for ^{220}Rn exhibits a pronounced peak close to the recoil energy of 103.4 keV that the radon nucleus gains from alpha decay of ^{224}Ra . Such a distribution shows that an essential part of ^{220}Rn nuclei escapes from the seed without scattering and accompanying energy loss. The physical reason for this is that parent ^{224}Ra nuclei are concentrated in the thin surface layer and emerging radon nuclei leave the seed without interacting with nuclei of seed material.

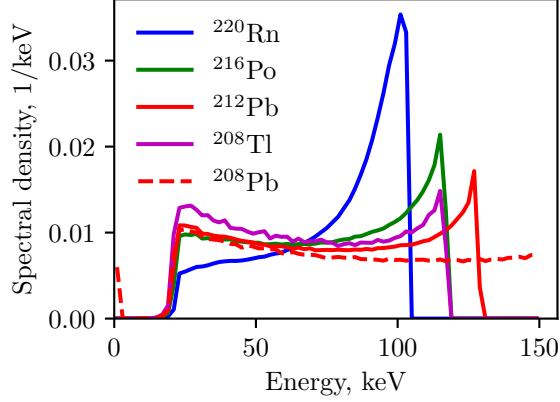


Figure 4: Spectra of the recoil nuclei escaping the DART seed

For other alpha decay products the peak around the recoil energy is less pronounced. This is the result of elastic scattering on the nuclei of the seed material that effectively lowers the energy of the moving nucleus. For the ^{208}Pb spectrum there is also a small peak at lower energies. This peak originates from ^{208}Pb nuclei emerging from beta decay of ^{208}Tl and having low recoil energy.

Recoil nuclei escaping the seed travel for some distance in tissue before they slow down to thermal energies. The further transport of these nuclei and their decay products in tissue is due to diffusive processes [5]. We did not consider diffusion and our simulation of nuclei transport in tissue included only the recoil nuclei emerging in the seed volume and entering the tissue. Also, during simulation radioactive decay of recoil nuclei traveling in tissue was prohibited. This is physically reasonable because half-life periods of radionuclides belonging to ^{224}Ra decay chain are considerably longer than typical times of recoil nuclei slowing down that could be estimated around 10^{-15} s.

Figure 5 shows distributions of recoil nuclei ranges in tissue obtained from Monte Carlo simulation. The corresponding average range values are presented in Table 3. One can see that recoil energy allows nuclei escaping the seed to travel to about 100 nm in tissue. The average ranges for all radionuclides from the decay chain except for ^{208}Pb have very close values of about approximately 30 nm. The obtained value is much smaller than the seed radius of 0.15 mm. This shows that for macroscopic models describing

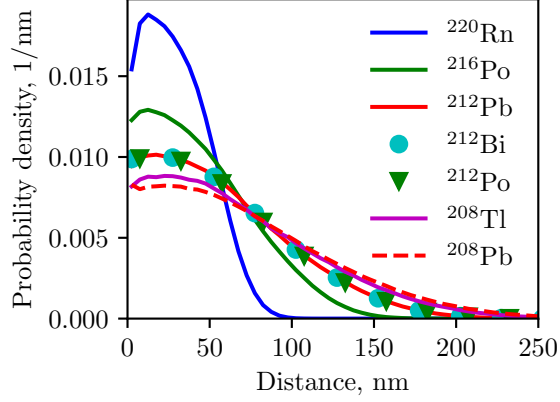


Figure 5: Distribution of recoil nuclei ranges in tissue

Nucleus	Distance, nm
^{220}Rn	30.3
^{216}Po	30.7
^{212}Pb	32.2
^{208}Tl	29.2
^{208}Pb	39.2

Table 3: Average recoil nuclei ranges in tissue

diffusion of ^{224}Ra decay products one can neglect the recoil nuclei penetration into the tissue and assume that they decay directly on the seed surface. However, if we are interested in the dose distribution near the seed surface such an assumption will be illegal.

Dose distribution around the seed is formed by coupled processes of radioactive decay and diffusion. The unstable recoil nuclei escaped from the seed are transported by diffusion and undergo radioactive decay during movement. The characteristic values of diffusion lengths obtained from macroscopic models are 0.3 mm for ^{220}Rn and 0.6 mm for ^{212}Pb , and radial dimensions of the region with therapeutic levels of alpha-particle dose is about 5-10 diffusion lengths [5].

At the same time ^{224}Ra and essential part of its decay products remain inside the seed. Alpha particles emerging from decays of these nuclei form dose distribution in the region close to the seed surface. This distribution

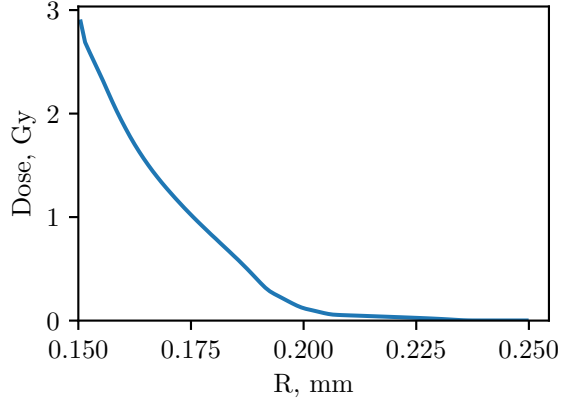


Figure 6: Dose distribution around the seed with radius of 0.15 mm from decays inside the seed, where R is radial distance from the seed axis. The initial ^{224}Ra activity is 3 μCi (111 kBq) and irradiation time is 10 days

could not be calculated within the macroscopic approach, so we used Monte Carlo simulation to calculate alpha-particles dose from decays inside the seed.

Radial dose distribution from alpha particles emerging inside the seed is shown in Figure 6. This distribution was calculated for a 1 cm long seed with initial activity of 3 μCi (111 kBq) and irradiation time of 10 days. The region where dose is formed by alpha particles leaving the seed extends approximately to 0.2 mm from the needle axis (0.05 mm from the surface). The size of this region is considerably smaller than the size of the treatment region which is around several millimeters [3].

The calculated dose distribution shows that close to the seed alpha-particles dose reaches the value of 2.9 Gy. Average dose in the region irradiated by alpha particles from the seed exceeds 0.49 Gy. This should be compared to the reference dose of 10 Gy used to define size of the treatment region [3]. One can see that alpha decays inside the DART seed make an essential contribution to the total dose and should be accounted for during treatment planning.

4. Conclusions

In this paper we examined the release of ^{224}Ra decay products from the DART seed due to nuclear recoil effect. Using Monte Carlo simulation we

calculated their desorption probabilities and showed that beside ^{220}Rn with desorption probability of 40%, release of ^{216}Po and ^{212}Pb with desorption probabilities of 15% and 12% respectively makes noticeable contribution to the dose to the tissue surrounding the seed. From the simulation we also obtained distribution of ^{224}Ra decay products remaining inside the seed and calculated dose to tissue from decays of these nuclei. This dose could exceed 2.9 Gy close to the seed surface for initial seed activity of 3 μCi (111 kBq) and irradiation time of 10 days. Under these conditions the average dose to the tissue layer with thickness of 0.05 mm exceeds 0.49 Gy.

The obtained results complement the existing macroscopic theory for the recoil nuclei transport [5]. They could be used for development of the improved macroscopic theory describing dynamics of ^{224}Ra decay products in tissue.

This research did not receive any specific grant from funding agencies in the public, commercial, or not-for-profit sectors.

References

- [1] P. E. Borchardt, R. R. Yuan, M. Miederer, M. R. McDevitt, D. A. Scheinberg, Targeted actinium-225 in vivo generators for therapy of ovarian cancer, *Cancer Research* 63 (16) (2003) 5084–5090.
- [2] R. M. De Kruijff, H. T. Wolterbeek, A. G. Denkova, A Critical Review of Alpha Radionuclide Therapy—How to Deal with Recoiling Daughters?, *Pharmaceuticals* 8 (2) (2015) 321–336. doi:10.3390/ph8020321.
- [3] L. Arazi, T. Cooks, M. Schmidt, Y. Keisari, I. Kelson, Treatment of solid tumors by interstitial release of recoiling short-lived alpha emitters, *Physics in Medicine and Biology* 52 (16) (2007) 5025–5042. doi:10.1088/0031-9155/52/16/021.
- [4] L. Arazi, T. Cooks, M. Schmidt, Y. Keisari, I. Kelson, The treatment of solid tumors by alpha emitters released from ^{224}Ra -loaded sources—internal dosimetry analysis, *Physics in Medicine and Biology* 55 (4) (2010) 1203–1218. doi:10.1088/0031-9155/55/4/020.
- [5] L. Arazi, Diffusing alpha-emitters radiation therapy: Approximate modeling of the macroscopic alpha particle dose of a point source,

Physics in Medicine & Biology 65 (1) (2020) 015015. doi:10.1088/1361-6560/ab5b73.

- [6] T. Cooks, M. Schmidt, H. Bittan, E. Lazarov, L. Arazi, I. Kelson, Y. Keisari, Local Control of Lung Derived Tumors by Diffusing Alpha-Emitting Atoms Released From Intratumoral Wires Loaded With Radium-224, *International Journal of Radiation Oncology, Biology, Physics* 74 (3) (2009) 966–973. doi:10.1016/j.ijrobp.2009.02.063.
- [7] A. Popovtzer, E. Rosenfeld, A. Mizrachi, S. R. Bellia, R. Ben-Hur, G. Feliciani, A. Sarnelli, L. Arazi, L. Deutsch, I. Kelson, Y. Keisari, Initial Safety and Tumor Control Results From a “First-in-Human” Multicenter Prospective Trial Evaluating a Novel Alpha-Emitting Radionuclide for the Treatment of Locally Advanced Recurrent Squamous Cell Carcinomas of the Skin and Head and Neck, *International Journal of Radiation Oncology, Biology, Physics* 106 (3) (2020) 571–578. doi:10.1016/j.ijrobp.2019.10.048.
- [8] S. Agostinelli, J. Allison, K. Amako, J. Apostolakis, H. Araujo, P. Arce, M. Asai, D. Axen, S. Banerjee, G. Barrand, F. Behner, L. Bellagamba, J. Boudreau, L. Broglia, A. Brunengo, H. Burkhardt, S. Chauvie, J. Chuma, R. Chytracek, G. Cooperman, G. Cosmo, P. Degtyarenko, A. Dell’Acqua, G. Depaola, D. Dietrich, R. Enami, A. Feliciello, C. Ferguson, H. Fesefeldt, G. Folger, F. Foppiano, A. Forti, S. Garelli, S. Giani, R. Giannitrapani, D. Gibin, J. J. Gómez Cadenas, I. González, G. Gracia Abril, G. Greeniaus, W. Greiner, V. Grichine, A. Grossheim, S. Guatelli, P. Gumplinger, R. Hamatsu, K. Hashimoto, H. Hasui, A. Heikkinen, A. Howard, V. Ivanchenko, A. Johnson, F. W. Jones, J. Kallenbach, N. Kanaya, M. Kawabata, Y. Kawabata, M. Kawaguti, S. Kelner, P. Kent, A. Kimura, T. Kodama, R. Kokoulin, M. Kossov, H. Kurashige, E. Lamanna, T. Lampén, V. Lara, V. Lefebure, F. Lei, M. Liendl, W. Lockman, F. Longo, S. Magni, M. Maire, E. Medernach, K. Minamimoto, P. Mora de Freitas, Y. Morita, K. Murakami, M. Nagamatu, R. Nartallo, P. Nieminen, T. Nishimura, K. Ohtsubo, M. Okamura, S. O’Neale, Y. Oohata, K. Paech, J. Perl, A. Pfeiffer, M. G. Pia, F. Ranjard, A. Rybin, S. Sadilov, E. Di Salvo, G. Santin, T. Sasaki, N. Savvas, Y. Sawada, S. Scherer, S. Sei, V. Sirotenko, D. Smith, N. Starkov, H. Stoecker, J. Sulkimo, M. Takahata, S. Tanaka, E. Tcherniaev, E. Safai Tehrani, M. Tropeano, P. Truscott, H. Uno,

- L. Urban, P. Urban, M. Verderi, A. Walkden, W. Wander, H. Weber, J. P. Wellisch, T. Wenaus, D. C. Williams, D. Wright, T. Yamada, H. Yoshida, D. Zschiesche, Geant4—a simulation toolkit, *Nuclear Instruments and Methods in Physics Research Section A: Accelerators, Spectrometers, Detectors and Associated Equipment* 506 (3) (2003) 250–303. doi:10.1016/S0168-9002(03)01368-8.
- [9] J. Allison, K. Amako, J. Apostolakis, H. Araujo, P. Arce Dubois, M. Asai, G. Barrand, R. Capra, S. Chauvie, R. Chytracsek, G. Cirrone, G. Cooperman, G. Cosmo, G. Cuttone, G. Daquino, M. Donszelmann, M. Dressel, G. Folger, F. Foppiano, J. Generowicz, V. Grichine, S. Guatelli, P. Gumplinger, A. Heikkinen, I. Hrivnacova, A. Howard, S. Incerti, V. Ivanchenko, T. Johnson, F. Jones, T. Koi, R. Kokoulin, M. Kossov, H. Kurashige, V. Lara, S. Larsson, F. Lei, O. Link, F. Longo, M. Maire, A. Mantero, B. Mascialino, I. McLaren, P. Mendez Lorenzo, K. Minamimoto, K. Murakami, P. Nieminen, L. Pandola, S. Parlati, L. Peralta, J. Perl, A. Pfeiffer, M. Pia, A. Ribon, P. Rodrigues, G. Russo, S. Sadilov, G. Santin, T. Sasaki, D. Smith, N. Starkov, S. Tanaka, E. Tcherniaev, B. Tome, A. Trindade, P. Truscott, L. Urban, M. Verderi, A. Walkden, J. Wellisch, D. Williams, D. Wright, H. Yoshida, Geant4 developments and applications, *IEEE Transactions on Nuclear Science* 53 (1) (2006) 270–278. doi:10.1109/TNS.2006.869826.
- [10] J. Allison, K. Amako, J. Apostolakis, P. Arce, M. Asai, T. Aso, E. Bagli, A. Bagulya, S. Banerjee, G. Barrand, B. R. Beck, A. G. Bogdanov, D. Brandt, J. M. C. Brown, H. Burkhardt, P. Canal, D. Cano-Ott, S. Chauvie, K. Cho, G. A. P. Cirrone, G. Cooperman, M. A. Cortés-Giraldo, G. Cosmo, G. Cuttone, G. Depaola, L. Desorgher, X. Dong, A. Dotti, V. D. Elvira, G. Folger, Z. Francis, A. Galoyan, L. Garnier, M. Gayer, K. L. Genser, V. M. Grichine, S. Guatelli, P. Guèye, P. Gumplinger, A. S. Howard, I. Hřivnáčová, S. Hwang, S. Incerti, A. Ivanchenko, V. N. Ivanchenko, F. W. Jones, S. Y. Jun, P. Kaitaniemi, N. Karakatsanis, M. Karamitros, M. Kelsey, A. Kimura, T. Koi, H. Kurashige, A. Lechner, S. B. Lee, F. Longo, M. Maire, D. Mancusi, A. Mantero, E. Mendoza, B. Morgan, K. Murakami, T. Nikitina, L. Pandola, P. Paprocki, J. Perl, I. Petrović, M. G. Pia, W. Pokorski, J. M. Quesada, M. Raine, M. A. Reis, A. Ribon, A. Ristić Fira, F. Romano, G. Russo, G. Santin, T. Sasaki, D. Sawkey, J. I. Shin,

- I. I. Strakovsky, A. Taborda, S. Tanaka, B. Tomé, T. Toshito, H. N. Tran, P. R. Truscott, L. Urban, V. Uzhinsky, J. M. Verbeke, M. Verderi, B. L. Wendt, H. Wenzel, D. H. Wright, D. M. Wright, T. Yamashita, J. Yarba, H. Yoshida, Recent developments in Geant4, *Nuclear Instruments and Methods in Physics Research Section A: Accelerators, Spectrometers, Detectors and Associated Equipment* 835 (2016) 186–225. doi:10.1016/j.nima.2016.06.125.
- [11] V. N. Ivanchenko, O. Kadri, M. Maire, L. Urban, Geant4 models for simulation of multiple scattering, *Journal of Physics: Conference Series* 219 (3) (2010) 032045. doi:10.1088/1742-6596/219/3/032045.
- [12] M. H. Mendenhall, R. A. Weller, Algorithms for the rapid computation of classical cross sections for screened Coulomb collisions, *Nuclear Instruments and Methods in Physics Research Section B: Beam Interactions with Materials and Atoms* 58 (1) (1991) 11–17. doi:10.1016/0168-583X(91)95672-Z.
- [13] M. H. Mendenhall, R. A. Weller, An algorithm for computing screened Coulomb scattering in Geant4, *Nuclear Instruments and Methods in Physics Research Section B: Beam Interactions with Materials and Atoms* 227 (3) (2005) 420–430. doi:10.1016/j.nimb.2004.08.014.
- [14] D. A. Brown, M. B. Chadwick, R. Capote, A. C. Kahler, A. Trkov, M. W. Herman, A. A. Sonzogni, Y. Danon, A. D. Carlson, M. Dunn, D. L. Smith, G. M. Hale, G. Arbanas, R. Arcilla, C. R. Bates, B. Beck, B. Becker, F. Brown, R. J. Casperson, J. Conlin, D. E. Cullen, M. A. Descalle, R. Firestone, T. Gaines, K. H. Guber, A. I. Hawari, J. Holmes, T. D. Johnson, T. Kawano, B. C. Kiedrowski, A. J. Koning, S. Kopecky, L. Leal, J. P. Lestone, C. Lubitz, J. I. Márquez Damián, C. M. Mattoon, E. A. McCutchan, S. Mughabghab, P. Navratil, D. Neudecker, G. P. A. Nobre, G. Noguere, M. Paris, M. T. Pigni, A. J. Plompen, B. Pritychenko, V. G. Pronyaev, D. Roubtsov, D. Rochman, P. Romano, P. Schillebeeckx, S. Simakov, M. Sin, I. Sirakov, B. Sleaford, V. Sobes, E. S. Soukhovitskii, I. Stetcu, P. Talou, I. Thompson, S. van der Marck, L. Welsch-Sherrill, D. Wiarda, M. White, J. L. Wormald, R. Q. Wright, M. Zerkle, G. Žerovnik, Y. Zhu, ENDF/B-VIII.0: The 8th Major Release of the Nuclear Reaction Data Library with CIELO-project Cross

Sections, New Standards and Thermal Scattering Data, Nuclear Data
Sheets 148 (2018) 1–142. doi:10.1016/j.nds.2018.02.001.